Decoding Neural Metabolic Markers From the Carotid Sinus Nerve in a Type 2 Diabetes Model

Marina Cracchiolo, Joana F. Sacramento, Alberto Mazzoni, Alessandro Panarese, Jacopo Carpaneto, Silvia V. Conde, and Silvestro Micera, *Senior Member, IEEE*

***Abstract*— Recent studies showed that the carotid sinus nerve (CSN) and the sympathetic nervous system (SNS) are overactivated in type 2 diabetes and that restoring the correct CSN neural activity can re-establish the proper metabolism. However, a robust characterization of the relationship between CSN and SNS neural activities and metabolism in type 2 diabetes is still missing. Here, we investigated the relationship between neural activity of CSN and SNS in control rats and in rats with diet-induced type 2 diabetes and the animal condition during metabolic challenges. We found that the diabetic condition can be discriminated on the basis of CSN and SNS neural activities due to a high-frequency shift in both spectra. This shift is suppressed in the SNS in case of CSN denervation, confirming the role of CSN in driving sympathetic overactivation in type 2 diabetes. Interestingly, the Inter-Burst-Intervals (IBIs) calculated from CSN bursts strongly correlate with perturbations in glycaemia levels. This finding, held for both control and diabetic rats, indicates the possibility of detecting metabolic information from neural recordings even in pathological conditions. Our results suggest that CSN activity could serve as a marker to monitor glycaemic alterations and, therefore, it could be used for closed-loop control of CSN neuromodulation. This paves the way to the development of novel and effective bioelectronic therapies for type 2 diabetes.**

***Index Terms*— Carotid sinus nerve, carotid sinus nerve resection, glucose intolerance, insulin resistance, sympathetic nervous system activity, type 2 diabetes.**

Manuscript received April 23, 2019; revised August 29, 2019 and September 13, 2019; accepted September 17, 2019. Date of publication September 23, 2019; date of current version October 8, 2019. This work was supported in part by Galvani Bioelectronics (formerly the Bioelectronics R&D Unit at GlaxoSmithKline) and in part by the Bertarelli Foundation. The work of J. F. Sacramento was supported by the Portuguese Foundation for Science and Technology through a Ph.D. Grant under Grant PD/BD/105890/2014. *(Joana F. Sacramento and Alberto Mazzoni contributed equally to this work.) (Corresponding authors: Silvia V. Conde; Silvestro Micera.)*

M. Cracchiolo, A. Mazzoni, A. Panarese, and J. Carpaneto are with The BioRobotics Institute, Scuola Superiore Sant'Anna, 56025 Pontedera, Italy (e-mail: m.cracchiolo@sssup.it; a.mazzoni@sssup.it; a.panarese@sssup.it; j.carpaneto@sssup.it).

J. F. Sacramento and S. V. Conde are with CEDOC, NOVA Medical School, Faculdade Ciências Médicas, 1150-082 Lisbon, Portugal (e-mail: joana.sacramento@nms.unl.pt; silvia.conde@nms.unl.pt).

S. Micera is with The BioRobotics Institute, Scuola Superiore Sant'Anna, 56025 Pontedera, Italy, and with the Bertarelli Foundation Chair in Translational NeuroEngineering, Center for Neuroprosthetics and Institute of Bioengineering, École Polytechnique Federale de Lausanne, CH-1202 Genève, Switzerland (e-mail: s.micera@sssup.it).

Digital Object Identifier 10.1109/TNSRE.2019.2942398

I. Introduction

THE autonomic nervous system is essential for the maintenance of body homoeostasis. The antagonistic effects of its sympathetic and parasympathetic divisions regulate several basic functions, including heart rate, breathing rate, and metabolism. Overactivation of the sympathetic nervous system (SNS) is an autonomic dysfunction associated with hypertension (HT) as well to insulin resistance (IR) and glucose intolerance, typical features of type 2 diabetes mellitus [1]–[4]. Studies suggest that SNS overactivity is related to the deregulation of the carotid bodies (CB), peripheral chemoreceptors located bilaterally at the bifurcation of the common carotid artery, and of its sensitive nerves, the carotid sinus nerves (CSN) (for a review see [5]). The CSN is a branch of the glossopharyngeal nerve which conveys information from both the CB and the baroreceptors of the carotid sinus. This double sensory innervation elicits opposite responses and inhibits each other in the solitary tract nucleus [6]. More in detail, the baroreceptor component leads to the sympathetic inhibition, decreasing blood pressure and leading to bradycardia, while the chemoreceptor component activates the sympathetic system [6]. Chemoreceptors in the CB are known to respond to hypoxia, hypercapnia, and acidosis [7], but have recently been also proposed to act as a metabolic sensor (see Conde *et al*. 2014 for a review) due to their sensitivity to insulin blood concentration and to the involvement in glucose homeostasis. Moreover, the CB and the CSN have been shown to be both overactivated in IR and HT animal models induced by hypercaloric diets [9], [10]. Supporting this hypothesis, CSN bilateral denervation was shown to prevent and reverse glucose intolerance, IR and HT as well as to avoid the increasing of sympathoadrenal activity in diet-induced prediabetic and type 2 diabetic rats [9], [11]. Unfortunately, surgical resection of the CSN is not a clinically usable solution since it produces side effects as the loss of the peripheral hypoxic response, decreased sensitivity to CO_2 [12], [13], impaired response to exercise [14]–[16] and fluctuations in blood pressure [17].

A recent work showed that chronic high-frequency bilateral electrical modulation (KHFAC) of CSN activity can be used to achieve a similar effect, since restores glucose tolerance and insulin sensitivity in a reversible way [18]. However, this approach can also generate negative side effects due to the

loss of chemoreceptor functions and information conveyed by baroreceptors.

An interesting and valuable alternative would be the development of closed-loop neuromodulation solutions to adjust in real-time the neural activity related to metabolism and re-establish, as much as possible, the natural condition. This closed-loop neuromodulation device could possibly lead to chronic disease treatment by means of miniaturized electronic devices for peripheral nerve stimulation [19], [20].

To be pursued, however, this approach requires a detailed description of the modifications of CSN neural activity related to metabolism or induced by type 2 diabetes.

Such newly acquired knowledge would allow the identification of a suitable way to decode metabolic information from the CNS, and to close the control loop in an effective way.

Few studies have recently been published on the decoding of neural markers from the activity of autonomic nerves, mainly from the vagus nerve (VN). Sevcencu *et al*. correlated neurograms from the left VN in pigs with the respiratory cycle [21] and blood pressure [22] or both [23] during baseline activity. Other studies in mice demonstrated that the neural signals recorded from the VN are cytokine-specific [24]. CSN signals related to metabolic conditions have been, so far, analysed only with biochemical tools and surgical manipulations, but no studies have been yet performed to identify informative neural markers. In this study, we therefore aimed at addressing this issue by evaluating and characterizing the normal and pathological neural response of CSN to metabolic stimuli. In particular, we described in both frequency and time domains the neural activities recorded in the CSN and in the cervical sympathetic nerve, during *in vivo*experiments performed in control rats (CTL), and rats with type 2 diabetes induced by high-fat/high-sucrose diet (HFHSu). Furthermore, we quantified the effect of bilateral CSN denervation on SNS activity in randomly selected HFHSu rats, revealing the neural signature of SNS overactivation previously observed in metabolic diseases [9], [11]. Finally, the relationship between CSN activity and glycaemia was also investigated to show the possibility of extracting neural markers of glucose temporal evolution.

II. Materials and Methods

A. Animals and Experimental Procedure

Experiments were performed in male Wistar rats (8-9 weeks old) obtained from the vivarium of the NOVA Medical School|Faculdade de Ciências Médicas, Universidade Nova de Lisboa, Lisboa, Portugal. After randomisation, the animals were divided into two groups: (1) the control group that fed a regular chow (7.4% fat, 17% protein and 75% carbohydrate (4 % sugar); Dietex International Limited, France) and (2) the high-fat high-sucrose (HFHSu) group that fed a 60% lipid-rich diet (61.6% fat + 20.3% carbohydrate + 19.1% protein; Mucedola, Milan, Italy) plus 35% sucrose (PanReac, Madrid, Spain) in drinking water during 14-15 weeks to induce a type 2 diabetes stage as previously described by Sacramento *et al.* [18]. This method has been previously validated as an early phase type 2 diabetes model [18], [25], as it produces insulin resistance, glucose intolerance, increased glycemia and serum insulin levels. Animals were kept under temperature and humidity control ($21 \pm 1°C$; $55 \pm 10\%$ humidity) with a 12 h light/12 h dark cycle. Body weight was recorded and food and liquid intake were monitored twice per week. Principles of laboratory care were followed in accordance with the European Union Directive for Protection of Vertebrates Used for Experimental and Other Scientific Ends (2010/63/EU). Experimental protocols were approved by the ethics committee of the NOVA Medical School|Faculdade de Ciências Médicas.

B. Bilateral CSN Resection Protocol

After 14 weeks of diet period, animals were evaluated for insulin sensitivity and glucose tolerance through an insulin tolerance test (ITT) and an oral glucose tolerance test (OGTT), respectively. Afterwards, the groups were randomly divided and animals were submitted to bilateral CSN resection under ketamine (30mg/kg)/xylazine (4mg/kg) anaesthesia and buprenorphine (10μg/kg) analgesia ($n = 10$) [9], [11]. The other animals were submitted to a sham procedure ($n = 13$).

C. Insulin and Glucose Tolerance Test

Insulin sensitivity was evaluated through an ITT [26] in conscious animals. Briefly, in overnight fasted animals blood glucose was measured prior and immediately after an intravenous insulin bolus (100 mU/kg,Humulin Regular, Lilly) in the tail vein. The decline in plasma glucose concentration was measured over a 15 min period. The constant rate for glucose disappearance (K_{ITT}) was calculated according with [26]. Glucose tolerance was evaluated through an oral glucose tolerance test. After an overnight fast, a bolus of glucose (2g/kg body weight, Sigma, Madrid, Spain) was administered by oral *gavage*. Blood samples were collected by tail snipping at regular intervals (0, 15, 30, 60, 120, and 180 min) and glucose levels were measured with a glucometer (Precision Xtra Meter, Abbott Diabetes Care, Portugal). If on the day of insulin sensitivity and glucose tolerance evaluation, animals exhibited any signs of high glycemic values, not due to the pathological condition, values were excluded for that time point.

D. Electrophysiological Recordings

After twenty-five weeks of diet, neural signals from CSN and sympathetic nervous system (SNS) from the superior cervical nerve were recorded on the right-side of the animal with hand-made silver hook electrodes (diameter = 0.25 mm) in animals anaesthetized with pentobarbital (60 mg/kg i.p.) (Fig. 1a). The electrode tip was in selective contact with the selected nerves and the open preparation was covered with mineral oil to better isolate from activity of nearby nerves and environmental noise. Note that we have chosen to record in the cervical sympathetic chain since our aim was to evaluate the effect on the overall sympathetic activity, and not a regional activity as if we recorded at renal, lumbar or splanchnic sympathetic nerves. CSN and SNS were recorded *in vivo* in

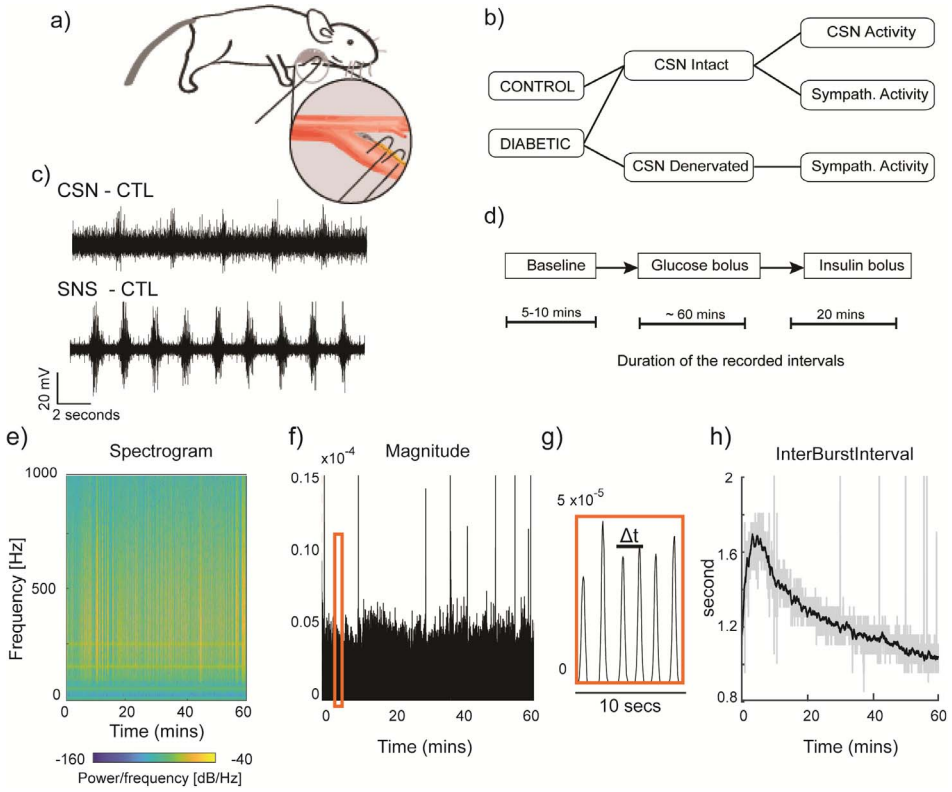

Fig. 1. Representative figure of carotid sinus nerve (CSN) recordings in vivo. a) Scheme of the rat with hook electrodes in the CSN. b) Group partitions of the recordings. c) Typical raw signal obtained from electrophysiological recordings of the CSN and SNS in a control rat. d) Timeline for all experimental sessions. E-h) Method to extract the Inter burst Interval (IBI): e) spectrogram computed on raw neural data recorded from the carotid sinus nerve. f) Magnitude of the spectrogram summed for each frequency over 300 Hz over a window size of sample 0.5 milliseconds with overlap of half the window length. g) Zoom in the 10 seconds orange window of panel f) to show magnitude peaks. h) Inter Burst Interval (IBI) obtained from the temporal distances between two following magnitude peaks. Grey line shows the raw IBI and the black line is the filtered IBI.

CSN-intact animals. Sympathetic activity was also recorded in CSN-denervated animals of the HFHsu diet group (Fig. 1b). No recordings of sympathetic activity were performed in the control denervated group since no changes in metabolic profile were observed (see Fig.2). Glycaemia levels and blood pressure were monitored throughout the experiment. Glucose levels were measured by tail tipping using a glucometer (Precision Xtra Meter, Abbott Diabetes Care, Portugal). CSN activity as well as sympathetic activity were recorded with a sampling rate at 20 kHz, amplified (Neurolog Digimiter, Hertfordshire, UK), band-pass filtered ([2 to 8000] Hz) and digitized (Axonscope, Axon Instruments, Molecular Devices, Wokingham, UK). Fig. 1c shows a typical raw signal obtained from electrophysiological recordings of the CSN.

E. Measuring Glucose and Insulin Administration Effects on CSN and SNS Neural Activity

Baseline activity for the CSN and SNS was recorded for 5-10 min. The effects of glucose and insulin on CSN and SNS activity were evaluated by recording the electrical activity of the nerves while performing glucose and insulin administrations in fasted animals (Fig. 1d). The glucose challenge was performed through an intravenous glucose tolerance test after the measurement of baseline levels. The test consisted in the administration of a glucose bolus (0.75 g/Kg body weight) in the femoral vein. Blood samples were taken from the tail vein at regular intervals (0, 2, 5, 8, 10, 15, 20, 30 min until the glycaemia fell to basal levels) and the neural signals were simultaneously recorded (for at least 30 minutes from the glucose bolus). As insulin is a stimulus for the carotid body and, as a consequence, for the carotid sinus nerve [8] we delivered insulin to the animal to investigate insulin effects on CSN and SNS neural activities. A bolus of insulin (100nM) was administered in the femoral vein and nerves were recorded for 20 minutes.

Additionally, to evaluate if the effect of the injection on neural activity was not due to volume administration, neural activity of the CSN and SNS was recorded after the administration of saline (NaCl, 0.9%) in the same volume than the used for glucose administration.

Femoral artery was catheterized to measure blood pressure and heart rate. The catheter was and connected to a pressure transducer (−50, +300 mmHg) and amplified (EMKA technologies, Paris, France).

F. Analysis of CSN and SNS Neural Activity

Spectral analysis of pre-processed electrophysiological data (see above) was performed as follows. Power supply noise at 50 Hz and its harmonics (from 50 to 2000 Hz) were removed with digital notch filters. Low-frequency artefacts and high-frequency noise were removed via a band-pass Butterworth

filter of the 4-th order with 50 Hz lower and 2 kHz upper cutoff frequencies.

The Power Spectrum (PS) was then computed with *pwelch* MATLAB function using 1-second windows and normalized to the overall power to obtain Power Spectrum Density (PSD). Herein, we used the PSD in all displayed analyses. Analysis of PS led to similar results but inter-session comparisons were slightly distorted due to the different amplitude of the recorded signals (data not shown).

To evaluate bursting activity in raw neural data, we first computed the spectrogram of the neural signal (*spectrogram* function in MATLAB, frequency range was [0 to 1000] Hz with a frequency step of 10 Hz) as shown in Figure 1e. Then, for each time value, we summed the magnitude of frequencies greater than 300 Hz, which is known to reflect the multiple-unit spiking activity [27] and we obtained a signal as in Fig.1f. Bursting activity was now clearly isolated from background activity and the temporal distances between two following bursts were measured (in seconds) (Fig.1g). Such signal, called Inter-Burst-Interval (IBI) (Fig. 1h), was then smoothed by means of a Hampel filter [28].

G. Statistical Analysis

Metabolic data were compared using GraphPad Prism Software, version 6 (GraphPad Software, La Jolla, CA, USA) and presented as mean values ± SEM. The statistical significance of the differences between the mean values was calculated by one- and two-way ANOVA with Bonferroni multiple comparison tests. Differences were considered significant at $p < 0.05$. Distributions of PSD values across diet groups are expressed as medians ± median confidence, where the latter is computed for the dataset X as in [29]:

$$\textit{median confidence}\ (X) = 1.57 * \frac{PR_{75}(X) - PR_{25}(X)}{\sqrt{|X|}} \quad (1)$$

Frequency intervals in which the PSD curves differ significantly across groups were found as follows: the power density associated to 50Hz-wide bins ranging from 75 Hz to 1975 Hz were considered for each curve. Then, significance of bin-wise differences was computed using a non-parametric Kruskal-Wallis test (KWT). In order to account for multiple comparisons, we performed a cluster-based permutation test (200 permutations generated) across different groups [30]. PSD peak values were compared across diet group and metabolic condition by means of a two-way ANOVA test [31].

In time domain, Pearson's coefficient, R, was used to seek for linear correlation between glycaemia and binned IBI (1-minute bin width). The linear relationship between these two variables was further investigated by a linear regression analysis. The reduced-CHI-squared, χ^2, was used to assess the goodness of fit. Differences were considered statistically significant for values $p < 0.05$. All the analyses on neural recordings were performed using MATLAB software (MathWorks, Natick, MA, USA).

III. Results

First, we assessed the effect of the hypercaloric diet and we characterized the effect the bilateral resection of the carotid sinus nerve. Then, the activity from the CSN and SNS nerves in type 2 diabetes and control rats was recorded to find neural markers of metabolic conditions (see Methods for details). Recordings were performed at baseline (fasted state) and following a successive delivery of a glucose bolus. As glucose levels returned to normoglycaemic values, approximately 90 minutes after the injection, insulin was administrated and the neural activity recorded for 20 minutes. The neural activity in the two groups was characterized by calculating the power spectrum density (PSD) and in the time-frequency domain (see Methods for details).

TABLE I
EFFECT OF CAROTID SINUS NERVE RESECTION ON THE AREA UNDER THE CURVE (AUC) OBTAINED FROM THE GLUCOSE EXCURSION CURVES OF ORAL GLUCOSE TOLERANCE TEST. TWO-WAY ANOVA WITH BONFERRONI MULTICOMPARISON TEST; $^{**}p < 0.01$ COMPARING AUC VALUES (MIN*MG/DL) BEFORE DIET VS 14 AND 25 WEEKS OF DIET; $^{\#\#}p < 0.01$ COMPARING VALUES BETWEEN 14 AND 25 WEEKS OF DIET

	Control	Control-denervation	HFHSu	HFHSu-denervation
Before diet	21848	21728	21625	21625
14 weeks diet	22169	22285	25389**	24949**
25 weeks diet	21953	21806	25151**	22529$^{\#\#}$

A. Effect of Diet and Bilateral CSN Resection on Insulin Sensitivity, Glucose Tolerance

Fig. 2 shows the effect of HFHSu diet and the effect of CSN bilateral resection on fasting glycaemia, insulin sensitivity and glucose tolerance. HFHSu diet during 14 weeks increased plasma fasting glycaemia to 100.33±1.91 mg/dl from a control value of 87.83±2.35 mg/dl. Eleven weeks after CSN resection, after 25 weeks of diet, fasting glycaemia was restored in HFHSu animals (87.83 ± 2.14 mg/dl) (Fig. 2a). Compared to controls, 14 weeks of HFHSu diet decreased insulin sensitivity by 42.12%, an effect that was completely restored 11 weeks after CSN resection (HFHSu CSN resection 25 weeks of diet KITT = 4.66 ± 0.37 %glucose/min) (Fig. 2b). CSN resection did not modify fasting glycaemia (Fig. 2a) or insulin sensitivity (Fig. 2b) in control animals. Additionally, HFHSu diet decreased glucose tolerance after 14 weeks of diet (Fig. 2c), as showed by the significant increase in the area under curve (AUC) of the glucose excursion curve in this group of animals (Table 1). Moreover, CSN resection restored glucose tolerance in HFHSu animals (Fig. 2c and Table 1).

B. Baseline Changes of Neural Activity in Type 2 Diabetes

First, we analyzed the baseline activity, i.e. the neural activity before administration of metabolic challenges, to assess diet-induced differences of spontaneous neural activity. Spectral analysis did not highlight a significant high frequency shift in PSD (KWT, $p > 0.05$; Fig. 3a) of CSN recordings from HFHSu animals compared to CTL, while there was a

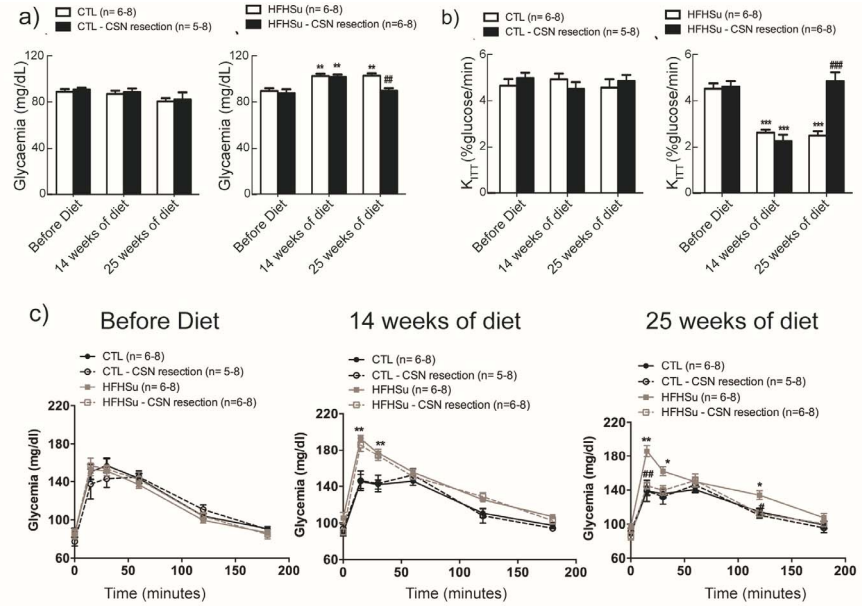

Fig. 2. Effect of high-fat-high-sucrose diet and carotid sinus nerve (CSN) resection on fasting glycaemia (a), insulin sensitivity (b) and glucose tolerance (c) in rats. (a) Effect of CSN resection on fasting glycaemia in control and HFHSu animals before diet, after 14 weeks of diet and after 25 weeks of diet; (b) effect of CSN resection on insulin sensitivity, expressed by the KITT, the constant of the insulin tolerance test in control and HFHSu animals before diet, after 14 weeks of diet and after 25 weeks of diet; (c) glucose excursion curves obtained through an oral glucose tolerance test in in control and HFHSu animals with and without CSN resection before diet, after 14 weeks of diet and after 25 weeks of diet. Values represent mean $\pm$ SEM. Two-Way ANOVA with Bonferroni multicomparison test, *p $<$ 0.05, **p $<$ 0.01 in comparison with control animals: ##p $<$ 0.01 in comparison with HFHSu animals.

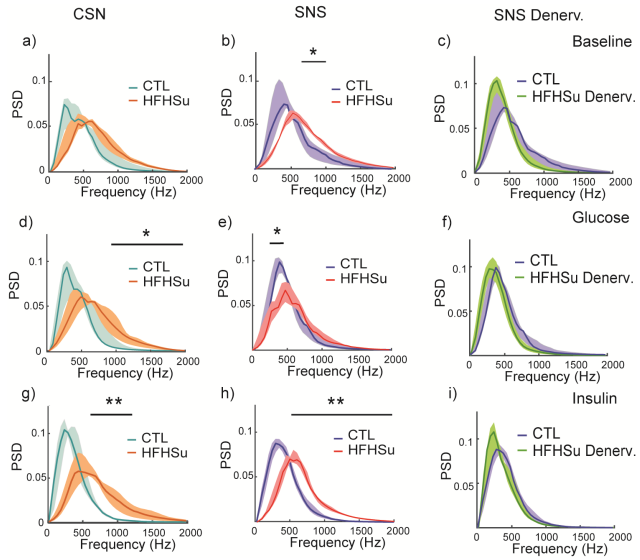

Fig. 3. Power Spectral Density in control rats, HFHSu rats and HFHSu rats with CSN-resection. Activity is recorded from the Carotid sinus nerve (CSN, left) or the sympathetic nervous system (SNS, center and right) during baseline, glucose challenge and insulin challenge. (a, d, g) Comparison between PSD of the CSN activity in control and HFHSu animals at baseline (a, N = 10 vs N = 10), after glucose injection (d, N = 8 vs N = 6) and after insulin injection (g, N = 5 vs N = 4). Here and in the following panels, tick lines indicate median and shaded areas indicate median confidence, and markers indicate significance difference between the two conditions (*p $<$ 0.05, **p $<$ 0.01 – KW test with Maris-Oostenveld correction). (b, e, h) Same as the first column for SNS in control and HFHSu animals (b, N = 5 vs N = 8; e, N = 9 vs N = 7; h, N = 5 vs N = 8). (c, f, i) same as the first column for SNS in control intact rats and HFHSu animals without CSN (c, N = 5 vs N = 4; f, N = 9 vs N = 6; i, N = 5 vs N = 4).

significant shift toward high frequencies in HFHSu animals in the spectra of signals recorded from SNS (KWT, p $<$ 0.05 in the range [600 to 950] Hz; Fig. 3b).

This result indicates that a high frequency shift in the PSD of sympathetic nerves is a signature of SNS overactivation associated with type 2 diabetes. This signature, however, is not directly detectable from the activity of CSN in baseline conditions.

C. Type 2 Diabetes-Induced Changes of Neural Activity After Glucose and Insulin Administration

We compared neural *in vivo* recordings from the CSN (Fig. 3, left column) in HFHSu vs. CTL animals to find whether hypercaloric diets/disease state produce detectable changes in CSN neural activity. Moreover, as several studies found evidences that SNS overactivity is involved in glucose metabolism deregulation, we wondered if we could directly measure such overactivity by recording and comparing SNS neural activity in both groups of animals (Fig. 3, middle column; see Methods for details).

We performed a two-way ANOVA on PSD peak positions of neural signals acquired in different conditions, depending on two factors: diet (HFHSu, CTL) and challenge (glucose injection, insulin injection and baseline). From the analysis of both CSN and SNS recordings, we found a significant role for the "diet" factor but no significant modulation due to factor "challenge" or "diet $\times$ challenge" interaction (CSN: challenge: p = 0.58; diet: p $<$ 0.01; challenge $\times$ diet: p = 0.57; SNS: challenge: p = 0.22; diet: p $<$ 0.01; challenge $\times$ diet: p = 0.52; CSN-denervated SNS: challenge: p = 0.15; diet: p $<$ 0.05; challenge $\times$ diet: p = 0.57).

We then looked at significant differences induced by "diet" for each challenge individually, looking not only at peak frequency, but also at differences in specific frequency bands.

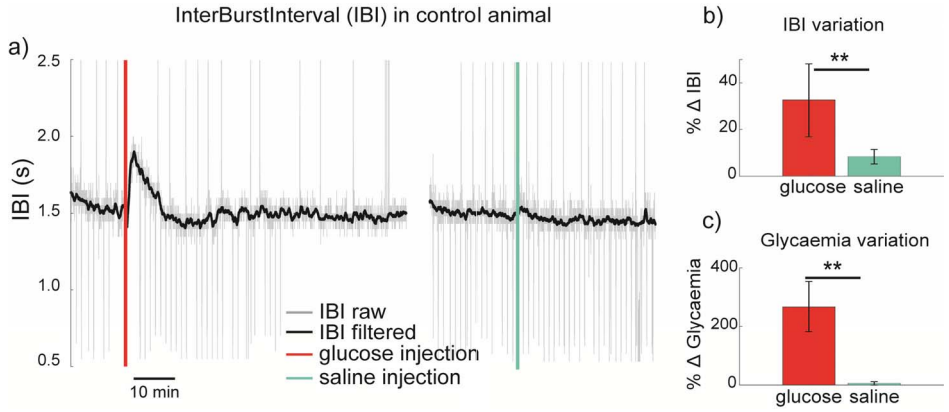

Fig. 4. Effect on interburst interval (IBI) in control rats after glucose and saline challenge. a) Raw and filtered IBI (grey and black tracks respectively) after glucose injection (red line) and saline injection (green line) in a control rat. IBI was computed from the raw neural signal of the carotid sinus nerve. b) Variation of the IBI in control rats due to saline (N = 6) and glucose (N = 8) administration. Delta was computed as the maximum excursion of IBI normalized to the minimum value. Bars represent the mean value across experiments and black lines indicate the standard deviation (**$p < 0.01$ – KW test). c) Same analysis as in panel b) for glycaemia excursion measured during the neural recording.

After glucose bolus, PSD of both CSN and SNS did show significant differences in the range [950 to 2000] Hz (KWT, $p < 0.05$ for this band, see Methods; Fig. 3d) and [200 to 400] Hz (KWT, $p < 0.05$ for this band, Fig. 3e), respectively. Also in the case of insulin injection, HFHSu animals displayed a neural activity with a stronger power than CTL in the range [550 to 1100] Hz for CSN (KWT $p < 0.01$ for this band; Fig. 3g) and [500 to 1950] Hz for SNS (KWT $p < 0.01$ for this band; Fig. 3h).

Taken together, all these results indicate that it is possible to discriminate between type 2 diabetes and control conditions thanks to an abnormal high frequency shift which can be found in the spectra of both SNS and CSN neural activities during metabolic challenges.

D. Effect of Bilateral CSN Resection on the Sympathetic Activity

Previous works [9], [11] studied metabolic consequences of CSN resection in type 2 diabetic rats but a comparative analysis of SNS neural activity after resection had never been performed. We investigated the effects of CSN resection on neural SNS activity of HFHSu and compared with CTL rats during baseline, glucose and insulin challenges. For glucose challenges, the SNS Denervated and CTL spectra were not significantly different (KWT $p > 0.15$ over the whole spectrum, Fig. 3f). In particular, the high-frequency activity shift induced in SNS by the diabetic state disappeared (compare with Fig. 3e).

As for glucose challenge, CSN denervation led to similar spectra for CTL and HFHSu SNS neural activity (KWT $p > 0.15$ over the whole spectrum; Fig. 3i) after insulin injection.

Overall these results, based on direct analysis of CSN and SNS neural activities, provides direct neural confirmation to conclusions drawn in previous works from biochemical markers, i.e.: i) type 2 diabetes is associated to SNS and CSN overactivity; ii) CSN resection leads to a SNS activity in HFHSu rats not different from CTL animals.

E. Neural Markers in CSN Correlate With Glycaemia Evolution

We then investigated the possibility to find a neural marker able to track, with a sufficiently high temporal precision, changes in the metabolic state of the subjects. In particular, we focused on the level of glycaemia, critical for people with type 2 diabetes. As CSN neural activity is characterized by large regular bursts (Fig. 1c), we looked for a possible relationship between bursting activity and glycaemia, focused on the interburst interval (or IBI; see Methods and Fig. 1).

In each experiment performed in control animals (N = 8), glucose i.v. administration was followed by a strong increase in glycaemia, as expected, but we also observed an increase in IBI.

To rule out the possibility that this increase was due to the injection *per se* or to changes in non-chemical physiological parameters, we performed a series of tests with saline injection (N = 6) in the same condition (fasted state, same volume). The example in Fig. 4a shows the effect of glucose and saline injection, respectively, in the same control animal. Saline did not cause any relevant excursion in the IBI (Δ mean value 8.3%) while the mean variation related to glucose bolus was 32.5% (Fig. 4b). As expected, saline injections did not lead to changes in glycaemia (Fig. 4c). This shows that IBI variation is due to the action of glucose/insulin.

We checked then if the correlation between glycaemia levels and IBI was strong enough to allow the reconstruction of glycemic temporal evolution starting from IBI (Fig. 5a). We first evaluated the cross correlation between IBI and glycaemia interpolated at IBI resolution (1 minute) for each single subject. A significant linear correlation between IBI and glycaemia was present in 7/8 control animals, with a fraction of explained variance as high as 98% (Fig. 5b and d). For each animal, the temporal lag related to the maximum value of the cross correlation is reported in Fig. 5c. If considering all animals together (after z-score normalization) linear correlation was still strong and highly significant ($R = 0.82$, $p << 0.001$; Fig. 5f). We then performed a linear regression analysis and

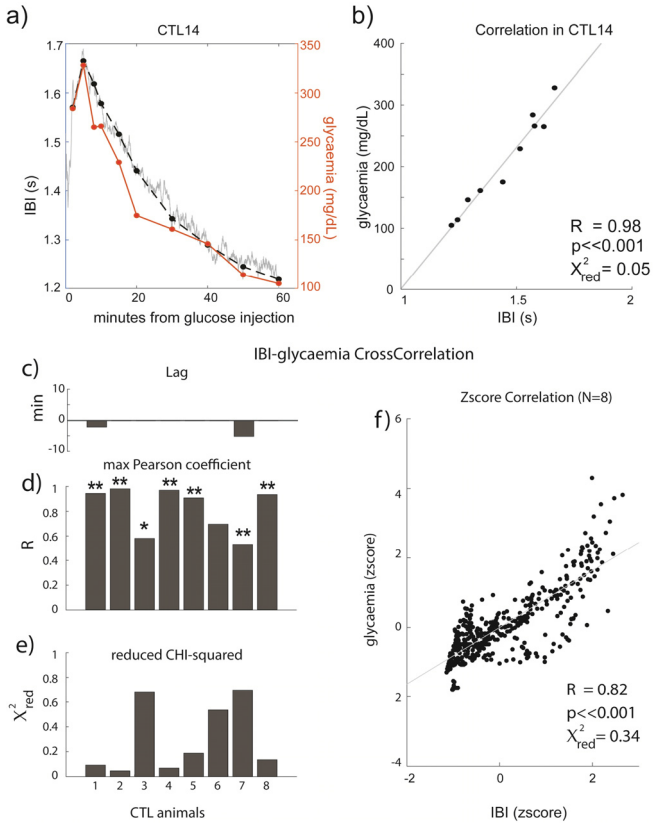

Fig. 5. Cross Correlation between interburst interval (IBI) and glycaemia after glucose injection in control rats. a) Evolution of glycaemia (red) and of IBI (black) downsampled at glucose measurements in a control animal. b) Scatterplot shows glycaemia values against IBI from panel a. The grey line represents the line of best fit. The value of R, i.e. the linear coefficient correlation, supported by the p value, and reduced-CHI-squared are reported. c-d) Temporal lag related to the maximum value of the cross correlation (c) and relative R supported by p values (d) for single experiments resulted from the correlation between IBI and glycaemia (*p $<$ 0.05, **p $<$ 0.01). e) Reduced-CHI-squared for single experiments for goodness of linear fit. f) Scatterplot related to IBI against glycaemia values for all the data from each experiment (N = 6) after zscore normalization, temporal shift and glycaemia interpolation. The grey line represents the line of best fit. R, supported by the p value, and reduced-CHI-squared are reported.

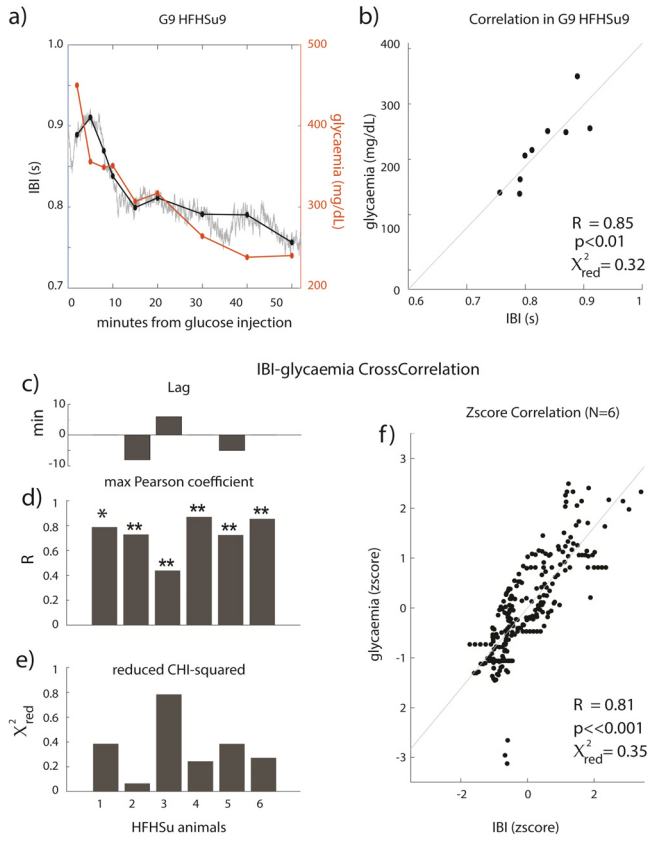

Fig. 6. Cross Correlation between interburst interval (IBI) and glycaemia after glucose injection in HFHSu rats. a) Evolution of glycaemia (red) and of IBI (black) downsampled at glucose measurements in a HFHSu animal. b) Scatterplot shows IBI against glycaemia values from panel a. The grey line represents the line of best fit. The value of R, i.e. the linear coefficient correlation, supported by the p value, and the reduced-CHI-squared is reported. c-d) Temporal lag related to the maximum value of the cross correlation (c) and relative R supported by p values (d) for single experiments resulted from the correlation between IBI and glycaemia (*p $<$ 0.05, **p $<$ 0.01). e) Reduced-CHI-squared for single experiments for goodness of linear fit. f) Scatterplot related to IBI against glycaemia values for all the data from each experiment (N = 6) after zscore normalization, temporal shift and glycaemia interpolation. The grey line represents the line of best fit. R, supported by the p value, and reduced-CHI-squared are reported.

found that reduced-CHI-squared, χ^2_{red}, computed on predicted values of glycaemia was shown to be consistently lower than 1 (Fig. 5e and f) indicating a very good quality of the fit.

Finally, we tested whether IBI was able to track changes in the metabolic state of diabetic animals as well, so we repeated the same analysis in HFHSu animals. We collected synchronous IBI values and interpolated glycaemia values after glucose injection (Fig. 6a and b). The Pearson correlation coefficient resulted significant for 6/6 experiments; the temporal lag related to the maximum value of the cross correlation is reported in Fig. 6c and d. As in the control group, the reduced-CHI-squared resulted lower than 1, assessing the goodness of the linear model (Fig. 6e). The overall correlation between normalized glycaemia and normalized IBI was significant (Fig. 6f) with R $=$ 0.81 and $\chi^2_{\text{red}} = 0.35$. Taken together, these results on CTL and HFHSu rats provide direct evidence that IBI extracted from the CSN neural activity is linearly correlated with glycaemia and could be used as a marker for the identification of changes in blood glucose levels, not only in healthy subjects, but also in diabetic ones.

IV. Discussion

Our results show that CSN neural activity carries information both to discriminate type 2 diabetic animals and to reconstruct on short timescale blood glucose level in both control and diabetic animals. This sheds new light on the neural modifications induced in the sympathetic nervous system by type 2 diabetes.

We observed for the first time the neural signature of CSN and SNS overactivation in type 2 diabetes, i.e. that the spectral content of CSN and SNS neural activities is shifted toward high frequencies. This provides new support to the hypothesis that both CSN and SNS recordings carry information about the metabolic status and strongly hints toward the possibility to discriminate the pathological condition. Additionally,

we found that the SNS high frequency shift was abolished in CSN-denervated HFHSu animals and this highlights the role of CB in the overactivation of the SNS previously suggested by [8], [9]. Finally, this work demonstrated a correlation between blood glucose levels and the interburst interval extracted from the CSN neural activity, suggesting that CSN recordings can function to monitor glycaemia evolution, not only in healthy subject but also in the case of the type 2 diabetes.

In these years, several studies looked for neural markers related to physiological and pathological states. In particular, the vagus nerve has been investigated and some neural features related to physiological activities as blood pressure, ventilation and inflammation have been found [21], [22], [24]. Here, instead, we focused on the CSN because it is directly involved in metabolism due to its innervation of the CB, which activates the SNS to regulate peripheral insulin sensitivity [9], [11]. We showed that both the healthy and the HFHSu groups revealed a high and reproducible correlation between CSN neural activity and glycaemia after glucose injection, while saline injection did not affect IBI, demonstrating that the effect on the *in vivo* CSN activity was produced by alterations in blood glucose concentrations and not by the injection *per se*.

In this work, we introduced new electrophysiological markers able to find significant differences between the neural activity of type 2 diabetic and healthy animals; these findings contribute to investigate the link between CB and SNS in glucose metabolism. Indeed, while the overactivation of the SNS is accepted as related to metabolic dysfunction, the involvement of the carotid body in glucose homeostasis was largely investigated in recent years [32] but only with biochemical and physiological data [9], [11], [33].

A. The Excitatory Role of the Carotid Body Related to Metabolism

It is known that CB chemoreceptor activity has an overall excitatory effect on SNS [8], [34], while baroreceptor activity has an overall inhibitory activity [12], [17], [35]. The net effect of the CSN inputs on SNS depends on the balance of CB chemoreceptors and carotid sinus activity. Our results support the hypothesis that the effect of CSN activity on SNS is mainly excitatory in the case of CB dysfunction when type 2 diabetes occurs [8]. We observed a significant frequency shift in both the CSN activity and the sympathetic tone, specific of the HFHSu condition (Figure 3, first and second columns). The excitatory relationship between CSN and SNS was also confirmed by the effect of CSN resection in HFHSu animals (Figure 3, third column), which leads to a decrease in SNS activity. This is coherent with the presence of a positive feedback loop involving CB insulin receptors, the sympathetic tone and insulin resistance [8]. Note that CSN spectrum overactivity would occur only when chemoreceptors are dominating, as in the condition of insulin resistance. This is expected in diabetic subjects, but might not happen in healthy subjects due to the correct balance between baro- and chemoreceptors activity [36], which inhibit each other in the nucleus of the solitary tract [6]. In the last decades, several studies have been performed to elucidate the role of the CB as a glucose sensor. However, this is still on debate as there is a lot of controversy in the results obtained by different research groups (for review see [8], [32]). In contrast, evidence has been provided showing that insulin activates the CB both in animals [37] and in humans [38]. Insulin receptors are present in the CB and phosphorylate in response to insulin promoting a neurosecretory response [9] that culminates in an increase in ventilation independently of hypoglycaemia [9], [37]. This increase in ventilation produced by insulin during euglycemia was also observed in humans [38]. Our results consolidated the role of the CB as a metabolic sensor if considered together with the findings that the CB is involved in the counterregulatory responses to hypoglycaemia [33] and in the genesis of metabolic diseases [9], [11]. However, to the best of our knowledge, no work has been done trying to find relationships between features from CSN recordings and *in vivo* metabolic parameters. Herein we showed, for the first time and *in vivo*, a correlation between CSN interburst interval with a metabolic feature such as glycaemia, both in control and type 2 diabetic animals (Figs. 5 and 6).

B. Limitations of This Study

Given the presence of different types of fibers in the CSN, we cannot rule out the possibility that part of the activity modulation observed in Figures 5 and 6 could be also due to the response of CSN baroreceptors. Recording only from the chemoreceptor fibers would be interesting but it is quite difficult due to the mixed (chemo/baro) nature of the nerves. Separating the chemo and baroreceptor fibers could be possible with mathematical tools as offline signal decomposition techniques [39]–[41]. However, for the purpose of biomedical application, what matters is that we were able to define metabolic neural markers in the whole CSN nerve without distinguishing between afferent and efferent fibers, especially because this characterization aims to future therapeutic applications asking for real-time processing approaches. In addition, we collected preliminary data to deal with possible confounds variables such as blood pressure and heart rate. This data suggested that IBI did not follow the same evolution of blood pressure or heart rate (Fig. 7) but further experiments will be necessary to assess the origin of IBI modulations. In fact, our results have been achieved in a controlled situation and under specific conditions, and they represent the first step towards a deep comprehension of the metabolic neural activity of the CSN. In particular, it would be interesting to investigate how respiratory correlates changes follow glucose alteration in other conditions including experiments in hypoxic/anoxic situation, or induced hyperventilation, and assess the sensitivity of IBI or the spectrum shift to other challenges, which could induce changes in the oxygen level or in the breathing frequency. However, a deeper understanding will be achievable with chronic recordings in freely moving awake animals because neurons can display significantly different magnitudes or patterns of discharge as function of animal status animal (e.g. depth of anesthesia, developmental stage and behavioral task). Major challenges for recordings in freely moving awake

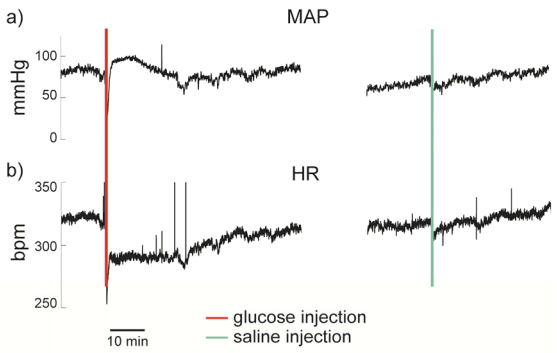

Fig. 7. Preliminary physiological data in control rats after glucose and saline challenge. a) Mean Arterial Pressure (MAP) after glucose injection (red line) and saline injection (green line) in a control rat. b) Heart rate (HR) after glucose injection (red line) and saline injection (green line) in a control rat.

animals are the quality of the recording electrodes, the level of noise associated with it and the approach used to perform the recording, e.g. use of tethered recording systems that can produce discomfort in the animal. Nevertheless, implantable and wireless multi-electrode array technologies have been developed and tested to record in freely moving animal, with a resolution comparable with in vivo anesthetized and in vivo conscious tethered recordings [42], [43].

C. Perspectives Toward Monitoring and Treating Type 2 Diabetes Through CSN Activity

Our results lay the ground for the development of an implantable medical device for the CSN to monitor and treat metabolic disorders. The implanted system should acquire the CSN activity and decode in real time the metabolic state by extracting IBI in type 2 diabetic subjects. Therefore, the device will be able to inform promptly type 2 diabetic subjects and caregivers of their metabolic condition and hence timely start suited actions if needed. This will be useful particularly for subjects that are unable to perform blood test due to age or concurring pathologies. Furthermore, we also anticipated that this metabolic monitoring unit could be a key part of a closed-loop mechanism of an implanted device aiming at selectively modulating whole-body metabolism through electrical activation/inhibition of the CSN or the autonomic nervous system. As mentioned above, Sacramento et al. described that continuous kilohertz frequency alternating current modulation of the CSN restored insulin sensitivity and glucose tolerance in type 2 diabetic rats [18]. However, the CSN is known to convey information related to the metabolic status but also with other functions as the regulation of blood pressure and the response to hypoxia [44]. For these reasons, a closed-loop approach working only when needed could bring significant improvement in the standard of care for type 2 diabetes.

V. Conclusion

Our motivation herein was to perform an in-depth analysis of CSN neural activity, both in control and pathological type 2 diabetic conditions, to evaluate its response to metabolic challenges. Spectral analysis provided important evidences about the overactivity of the CSN and SNS in type 2 diabetes and discriminated the pathological condition from the healthy one based on the neural activity. Moreover, our results lead us to propose IBI as a neural marker for whole-body glycaemia, demonstrating the possibility to design closed-loop neuroprosthetic devices oriented to monitor glucose level in subjects with type 2 diabetes starting from neural markers, which could be combined with the electrical stimulation to modulate CSN activity [18].

Acknowledgment

The authors want to acknowledge to Ms Bernardete Melo from Silvia Conde's Group at CEDOC, NOVA Medical School for the help in the metabolic evaluation of the animals. They thank Khatia Gabisonia for her helpful comments. Prof. Silvestro Micera and Prof. Silvia Conde are the guarantors of the study.

References

[1] G. F. DiBona, "Sympathetic nervous system and hypertension," *Hypertension*, vol. 61, no. 3, pp. 556–560, Mar. 2013.
[2] S. C. Malpas, "Sympathetic nervous system overactivity and its role in the development of cardiovascular disease," *Physiol. Rev.*, vol. 90, no. 2, pp. 513–557, Apr. 2010.
[3] G. W. Lambert, N. E. Straznicky, E. A. Lambert, J. B. Dixon, and M. P. Schlaich, "Sympathetic nervous activation in obesity and the metabolic syndrome—Causes, consequences and therapeutic implications," *Pharmacol. Therapeutics*, vol. 126, no. 2, pp. 159–172, May 2010.
[4] A. A. Thorp and M. P. Schlaich, "Relevance of sympathetic nervous system activation in obesity and metabolic syndrome," *J. Diabetes Res.*, vol. 2015, Mar. 2015, Art. no. 341583.
[5] R. Iturriaga, "Translating carotid body function into clinical medicine," *J. Physiol.*, vol. 596, no. 15, pp. 3067–3077, Aug. 2018.
[6] A. Porzionato, V. Macchi, C. Stecco, and R. De Caro, "The carotid sinus nerve—Structure, function, and clinical implications," *Anat. Rec.*, vol. 302, pp. 575–587, May 2018.
[7] C. Gonzalez, L. Almaraz, A. Obeso, and R. Rigual, "Carotid body chemoreceptors: From natural stimuli to sensory discharges," *Physiol. Rev.*, vol. 74, no. 4, pp. 829–898, Oct. 1994.
[8] S. V. Conde *et al.*, "Carotid body, insulin, and metabolic diseases: Unraveling the links," *Front. Physiol.*, vol. 5, p. 418, Oct. 2014.
[9] M. J. Ribeiro, J. F. Sacramento, C. Gonzalez, M. P. Guarino, E. C. Monteiro, and S. V. Conde, "Carotid body denervation prevents the development of insulin resistance and hypertension induced by hypercaloric diets," *Diabetes*, vol. 62, no. 8, pp. 2905–2916, Aug. 2013.
[10] S. V. Conde, J. F. Sacramento, and M. P. Guarino, "Carotid body: A metabolic sensor implicated in insulin resistance," *Physiol. Genomics*, vol. 50, no. 3, pp. 208–214, Mar. 2018.
[11] J. F. Sacramento *et al.*, "Functional abolition of carotid body activity restores insulin action and glucose homeostasis in rats: Key roles for visceral adipose tissue and the liver," *Diabetologia*, vol. 60, no. 1, pp. 158–168, Jan. 2017.
[12] H. J. L. M. Timmers, W. Wieling, J. M. Karemaker, and J. W. M. Lenders, "Denervation of carotid baro- and chemoreceptors in humans," *J. Physiol.*, vol. 553, no. 1, pp. 3–11, Nov. 2003.
[13] A. Dahan, D. Nieuwenhuijs, and L. Teppema, "Plasticity of central chemoreceptors: Effect of bilateral carotid body resection on central CO_2 sensitivity," *PLoS Med.*, vol. 4, no. 7, Jul. 2007, Art. no. e239.
[14] H. V. Forster, L. G. Pan, G. E. Bisgard, R. P. Kaminski, S. M. Dorsey, and M. A. Busch, "Hyperpnea of exercise at various PIO2 in normal and carotid body-denervated ponies," *J. Appl. Physiol.*, vol. 54, no. 5, pp. 1387–1393, May 1983.
[15] H. V. Forster and L. G. Pan, "The role of the carotid chemoreceptors in the control of breathing during exercise," *Med. Sci. Sports Exerc.*, vol. 26, no. 3, pp. 328–336, Mar. 1994.
[16] J. A. Dempsey and C. A. Smith, "Do carotid chemoreceptors inhibit the hyperventilatory response to heavy exercise?" *Can. J. Appl. Physiol.*, vol. 19, no. 3, pp. 350–359, Sep. 1994.
[17] J. F. Paton *et al.*, "The carotid body as a therapeutic target for the treatment of sympathetically mediated diseases," *Hypertension*, vol. 61, no. 1, pp. 5–13, Jan. 2013.

[18] J. F. Sacramento *et al.*, "Bioelectronic modulation of carotid sinus nerve activity in the rat: A potential therapeutic approach for type 2 diabetes," *Diabetologia*, vol. 61, no. 3, pp. 700–710, Mar. 2018.
[19] K. Famm, B. Litt, K. J. Tracey, E. S. Boyden, and M. Slaoui, "Drug discovery: A jump-start for electroceuticals," *Nature*, vol. 496, no. 7444, pp. 159–161, 2013.
[20] S. Reardon, "Electroceuticals spark interest," *Nature*, vol. 511, no. 7507, p. 18, Jul. 2014.
[21] C. Sevcencu, T. N. Nielsen, B. Kjærgaard, and J. J. Struijk, "A respiratory marker derived from left vagus nerve signals recorded with implantable cuff electrodes," *Neuromodulation, Technol. Neural Interface*, vol. 21, no. 3, pp. 269–275, Apr. 2018.
[22] C. Sevcencu, T. N. Nielsen, and J. J. Struijk, "A neural blood pressure marker for bioelectronic medicines for treatment of hypertension," *Biosensors Bioelectron.*, vol. 98, pp. 1–6, Dec. 2017.
[23] C. Sevcencu, T. N. Nielsen, and J. J. Struijk, "An intraneural electrode for bioelectronic medicines for treatment of hypertension," *Neuromodulation Technol. Neural Interface*, vol. 21, no. 8, pp. 777–786, Dec. 2018.
[24] T. P. Zanos *et al.*, "Identification of cytokine-specific sensory neural signals by decoding murine vagus nerve activity," *Proc. Nat. Acad. Sci. USA*, vol. 115, no. 21, pp. E4843–E4852, May 2018.
[25] B. F. Melo *et al.*, "Evaluating the impact of different hypercaloric diets on weight gain, insulin resistance, glucose intolerance, and its comorbidities in rats," *Nutrients*, vol. 11, no. 6, p. 1197, May 2019.
[26] S. V. Conde, T. N. da Silva, C. Gonzalez, M. M. Carmo, E. C. Monteiro, and M. P. Guarino, "Chronic caffeine intake decreases circulating catecholamines and prevents diet-induced insulin resistance and hypertension in rats," *Brit. J. Nutrition*, vol. 107, no. 1, pp. 86–95, Jan. 2012.
[27] M. M. Morgan *et al.*, "Multiunit activity," in *Encyclopedia Psychopharmacology*, I. P. Stolerman, Ed. Berlin, Germany: Springer, 2010, p. 809.
[28] R. K. Pearson, Y. Neuvo, J. Astola, and M. Gabbouj, "Generalized Hampel filters," *EURASIP J. Adv. Signal Process.*, vol. 2016, p. 87, Dec. 2016.
[29] J. M. Chambers, Ed., *Graphical Methods for Data Analysis*. Pacific Grove, CA, USA: Wadsworth, 1983.
[30] E. Maris and R. Oostenveld, "Nonparametric statistical testing of EEG- and MEG-data," *J. Neurosci. Methods*, vol. 164, no. 1, pp. 177–190, 2007.
[31] M. Cracchiolo *et al.*, "High frequency shift in carotid sinus nerve and sympathetic nerve activity in type 2 diabetic rat model," in *Proc. 9th Int. IEEE/EMBS Conf. Neural Eng. (NER)*, San Francisco, CA, USA, Mar. 2019, pp. 498–501.
[32] M. J. Joyner, J. K. Limberg, E. A. Wehrwein, and B. D. Johnson, "Role of the carotid body chemoreceptors in glucose homeostasis and thermoregulation in humans," *J. Physiol.*, vol. 596, no. 15, pp. 3079–3085, Apr. 2018.
[33] Y. Koyama *et al.*, "Evidence that carotid bodies play an important role in glucoregulation *in vivo*," *Diabetes*, vol. 49, no. 9, pp. 1434–1442, Sep. 2000.
[34] J. M. Marshall, "Peripheral chemoreceptors and cardiovascular regulation," *Physiol. Rev.*, vol. 74, no. 3, pp. 543–594, Jul. 1994.
[35] P. L. Katayama, J. A. Castania, D. P. M. Dias, K. P. Patel, R. Fazan, and H. C. Salgado, "Role of chemoreceptor activation in hemodynamic responses to electrical stimulation of the carotid sinus in conscious rats," *Hypertension*, vol. 66, no. 3, pp. 598–603, Sep. 2015.
[36] R. M. Berne, B. M. Koeppen, and B. A. Stanton, Eds., *Berne & Levy Physiology*, 6th ed. Philadelphia, PA, USA: Mosby, 2010.
[37] I. Bin-Jaliah, P. D. Maskell, and P. Kumar, "Indirect sensing of insulin-induced hypoglycaemia by the carotid body in the rat," *J. Physiol.*, vol. 556, no. 1, pp. 255–266, Apr. 2004.
[38] T. C. Barbosa *et al.*, "Insulin increases ventilation during euglycemia in humans," *Amer. J. Physiol.-Regulatory, Integrative Comparative Physiol.*, vol. 315, no. 1, pp. R84–R89, Mar. 2018.
[39] S. G. Mallat, "A theory for multiresolution signal decomposition: The wavelet representation," *IEEE Trans. Pattern Anal. Mach. Intell.*, vol. 11, no. 7, pp. 674–693, Jul. 1989.
[40] A. Hyvarinen, J. Karhunen, and E. Oja, *Independent Component Analysis*. New York, NY, USA: Wiley, 2001.
[41] M. Ester, H.-P. Kriegel, J. Sander, and X. Xu, "A density-based algorithm for discovering clusters a density-based algorithm for discovering clusters in large spatial databases with noise," in *Proc. 2nd Int. Conf. Knowl. Discovery Data Mining*, vol. 96, Aug. 1996, pp. 226–231.
[42] D. Fan *et al.*, "A wireless multi-channel recording system for freely behaving mice and rats," *PLoS ONE*, vol. 6, no. 7, Jul. 2011, Art. no. e22033.
[43] H. Xu, A. Weltman, K. Scholten, E. Meng, T. W. Berger, and D. Song, "Chronic multi-region recording from the rat hippocampus *in vivo* with a flexible Parylene-based multi-electrode array," in *Proc. 39th Annu. Int. Conf. IEEE Eng. Med. Biol. Soc. (EMBC)*, Seogwipo, South Korea, Jul. 2017, pp. 1716–1719.
[44] S. V. Conde, "Ablation of the carotid bodies in disease: Meeting its adverse effects," *J. Physiol.*, vol. 596, no. 15, p. 2955, Aug. 2018.